Globally optimal band structure for thermoelectrics in realistic systems

Junsoo Park ![ORCID]*

KBR, Inc., Intelligent Systems Division, NASA Ames Research Center, Moffett Field, California 94035, USA

The observation is made that a linear dispersion in any dimension under acoustic-phonon- deformation-potential scattering theoretically prescribes a constant charge transport distribution, required for the boxcar profile known to maximize the thermoelectric figure of merit. A linear dispersion squeezed by two transport gaps for optimized bandwidth under scattering by phonon deformation then theoretically constitutes a globally optimal qualitative band structure that may arise in real systems.

I. INTRODUCTION

In electron band transport, the charge transport distribution $\Sigma(E)$ (a.k.a. spectral conductivity, energy-dependent conductivity, transmission function) determines key properties such as Ohmic conductivity, the Seebeck coefficient, and electronic thermal conductivity. It is known that a boxcar-shaped $\Sigma(E)$ for given magnitude delivers optimal thermoelectric figure of merit zT in quantum systems obeying the Landauer-Büttiker transport formalism [1,2] as well as the semiclassical Boltzmann transport equations (BTE) under the relaxation time approximation [3,4]. The latter has recently been derived by exact mathematics [4]. Under BTE, $\Sigma_x(E) = \frac{1}{V}\langle v_x^2(E)\rangle D(E)\tau(E)$, where V is the system volume, x is a Cartesian direction, $\langle v_x^2 \rangle$ is the squared group velocity averaged over constant energy surface, D is the density of states, and τ is the lifetime, or inverse of the scattering rate τ^{-1}. A boxcar function, shown in Fig. 1(a), is essentially a Heaviside step function with an upper cutoff just like the lower one. Within their confines, the profile is constant and flat, or $\Sigma(E) = \Sigma^{\dagger} \propto E^0$. The ultimate question yet to be answered is what, if any, realistic bulk band structures and systems may physically achieve this and deliver optimal thermoelectric performance. It is herein observed that linear dispersion, in any dimension, under scattering by acoustic phonon deformation meets the theoretical requirement for realizing this goal.

II. LINEAR DISPERSION UNDER DEFORMATION-POTENTIAL SCATTERING

Table I summarizes the E dependence of $\langle v_x^2(E)\rangle$ and $D(E)$ of isotropic parabolic and linear dispersions in one, two, and three dimensions, along with the required E dependence of $\tau(E)$ and the corresponding $D(E)$ dependence of $\tau^{-1}(E)$ to enforce $\Sigma(E) \propto E^0$. No parabolic case is realistic, as they require $\tau^{-1}(E)$ profiles that do not match, even approximately, with any known electron-scattering mechanism. In turn, all of the linear cases, which exhibit $\langle v_x^2(E)\rangle \propto E^0$, require

that $\tau^{-1}(E) \propto D^1(E)$, the very behavior of deformation-potential scattering by long-wavelength longitudinal acoustic phonons—this has been derived not only for spherical Fermi surfaces of parabolic bands specifically [5–8] but also for an arbitrary Fermi surface around some band minimum [9,10]. More generally, consider a d-dimensional dispersion of order p. It is straightforward to show $\langle v^2(E)\rangle \propto E^{2(p-1)/p}$ and $D(E) \propto E^{(d/p)-1}$. The scattering behavior required to enforce $\Sigma(E) \propto E^0$ then is $\tau^{-1}(E) \propto E^{(p+d-2)/p}$, or in a more useful form, $\tau^{-1}(E) \propto D(E)E^{2(p-1)/p}$. The only realistic solution is $p = 1$, or linear dispersion, regardless of dimension under acoustic-deformation-potential scattering. This solution is as consequential as it is simple because linear dispersion is common and acoustic-deformation-potential scattering is ubiquitous in real materials.

To ascertain the need for deformation-potential scattering, consider the generalized deformation potential derived by Kahn and Allen [11], whose tensor form is

$$\mathbf{\Delta_k} = \mathbf{\Delta_k^0} + \mathbf{v_k} \otimes \mathbf{v_k}, \tag{1}$$

where $\mathbf{v}$ is the group-velocity vector, and Δ^0 the usual Bardeen-Shockley term [12] representing the strain-driven energy shift of bands. Note that the second, correction term does not contribute any energy dependence for linear bands since $\langle\mathbf{v}\rangle$ is a constant of energy. Since Δ is essentially energy independent for a single band, the scattering rate is guaranteed to behave as $\tau^{-1}(E) \propto D^1(E)$ due to the near elasticity of the process. Equation (1) has been implemented in the AM-SET software [13] and has led to very good agreements with experimentally measured transport properties for numerous materials. Though optical and high-wave-vector phonon deformations can introduce some inelasticity in real systems, first-principles calculations of full electron-phonon scattering in three [14–16] and two [17,18] dimensions, as well as other analyses [19], have demonstrated that the $\tau^{-1}(E) \propto D^1(E)$ trend persists for scattering due to phonon deformation, as phonon energies are typically small in the electronic energy scale. Other common processes, such as polar-optical or ionized-impurity scattering in semiconductors, are not known to exhibit as consistently simple E-or-$D(E)$

*junsoo.park@nasa.gov

(a) $\Sigma(E) = v^2(E)\tau(E)D(E)$
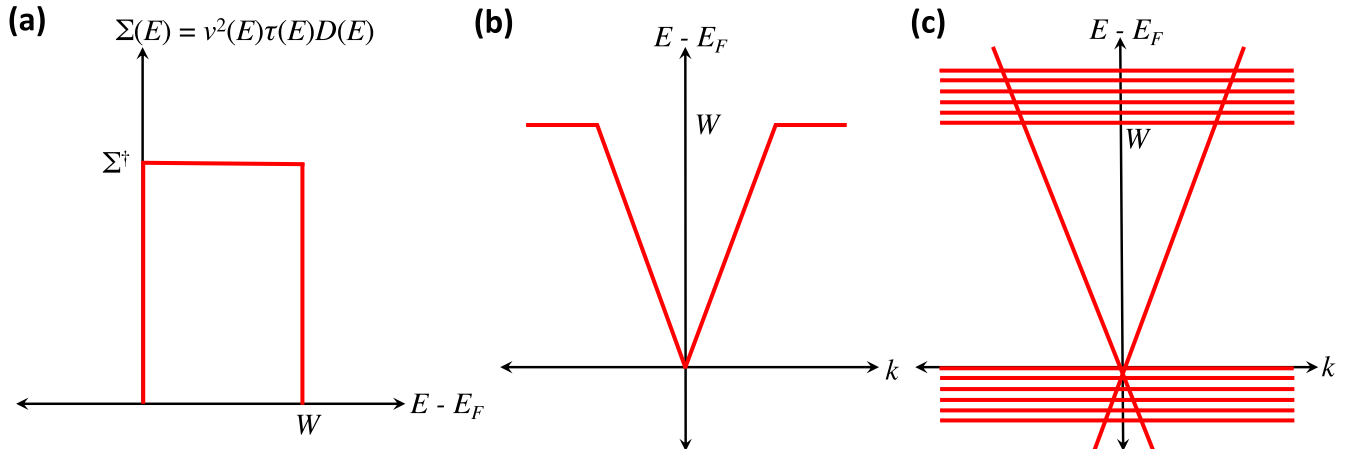
(b)

(c)

FIG. 1. (a) A boxcar transport distribution. (b) Schematic of the ideal band structure achieving a boxcar transport distribution with a band gap and high-energy cutoff. (c) Semimetallic schematic where transport cutoffs are achieved by resonant scattering states. All diagrams are from the *n*-type perspective where an electron dominates transport as opposed to a hole. The energy axes are zero referenced to the Fermi level for the sake of graphics, which in practice is an optimization parameter.

dependence of rates. The former has discontinuities at polar-optical phonon energies with different preemission and postemission behaviors, while the latter has a logarithmic screening term [6,10,20]. As such, they cannot be expected to pair with a simple realistic band to robustly yield $\Sigma(E) \propto E^0$.

III. OPTIMUM BANDWIDTH AND zT

The $\Sigma(E) \propto E^0$ profile is of course only one of the three requirements for realizing a boxcar function. The second requirement is a lower cutoff, and ideally a band gap would guarantee it as in Fig. 1(b). Unfortunately, a true linear dispersion would be gapless, forming a Dirac cone at the Fermi level with symmetric dispersion on the other side, triggering bipolar transport that suppresses thermopower. The dispersion would therefore need to develop a finite curvature at its utmost tip, similar to a Kane band [21,22] with a huge nonparabolicity parameter. In this semiconducting case, for polar-optical scattering to be a nonfactor, the material would preferably be nonpolar. If polar, its dielectric constant must have a tiny ionic part, or the operation temperature must be below that

seriously activates polar phonons. If the degeneracy at the Dirac point cannot be lifted, then the viable picture is for the opposing carrier type to be suppressed in τ to near-zero values by scattering into heavy resonancelike states, as in Fig. 1(c). This concept has been demonstrated in real semimetals with linear dispersion with heavy-band crossings [16,18], if not quite so ideally as here because the heavy states are not so flat and inelastic scattering slightly broadens the resolution of the boxcar edge. Nevertheless, considering the generally low phonon energies ($\lesssim 30$ meV for decent thermoelectrics) in the energy scale of electronic bands ($\lesssim 1$ eV), only the states close to the resonance states would be affected. The lower cutoff alone creates a Heaviside $\Sigma(E)$, which would be optimal for the power factor but not zT [4].

The third and final requirement for completing the boxcar is an upper cutoff. The reason for this is that, whereas the power factor does not concern electronic thermal conductivity (κ_e), zT does, and high-energy states contribute more to thermal conduction than charge conduction compared to low-energy states in relative terms. Shutting down the transport of high-energy carriers is especially relevant when $\kappa_e > \kappa_{lat}$, that is, when κ_{lat} is low and κ_e and the PF are high, precisely the condition for high performance. For this to happen, there would ideally exist another energy gap at W with the linear dispersion discontinuously flattening out, as in Fig. 1(b), though realistically the flattening would be abrupt at best. Perhaps a more viable picture is for efficient scattering states to be present or introduced so that τ is essentially zeroed out above W mirroring the low-energy resonance states, as in Fig. 1(c). In either case, the resulting bandwidth W is an important optimization parameter as investigated in Ref. [23] and is narrower at lower lattice thermal conductivity (κ_{lat}) and higher velocity. The theoretical optimum bandwidth (W_{opt}) and the corresponding maximal zT for linear dispersion under deformation-potential scattering are shown in Fig. 2. W_{opt} is obtained by the approach used in Ref. [23], solving for

TABLE I. Energy dependence of intrinsic isotropic band structure features as well as that of lifetimes and the causal carrier scattering rates required for enforcing $\Sigma(E) \propto E^0$.

Parabolic	$\langle v_x^2(E) \rangle$	$D(E)$	$\tau(E)$	$\tau^{-1}(E)$	$\Sigma_x(E)$
1D		$E^{-1/2}$	$E^{-1/2}$	$D^{-1}(E)$	
2D	E^1	E^0	E^{-1}	$D^\infty(E)$	E^0
3D		$E^{1/2}$	$E^{-3/2}$	$D^3(E)$	
Linear	$\langle v_x^2(E) \rangle$	$D(E)$	$\tau(E)$	$\tau^{-1}(E)$	$\Sigma_x(E)$
1D		E^0	E^0	$D^1(E)$	
2D	E^0	E^1	E^{-1}	$D^1(E)$	E^0
3D		E^2	E^{-2}	$D^1(E)$	

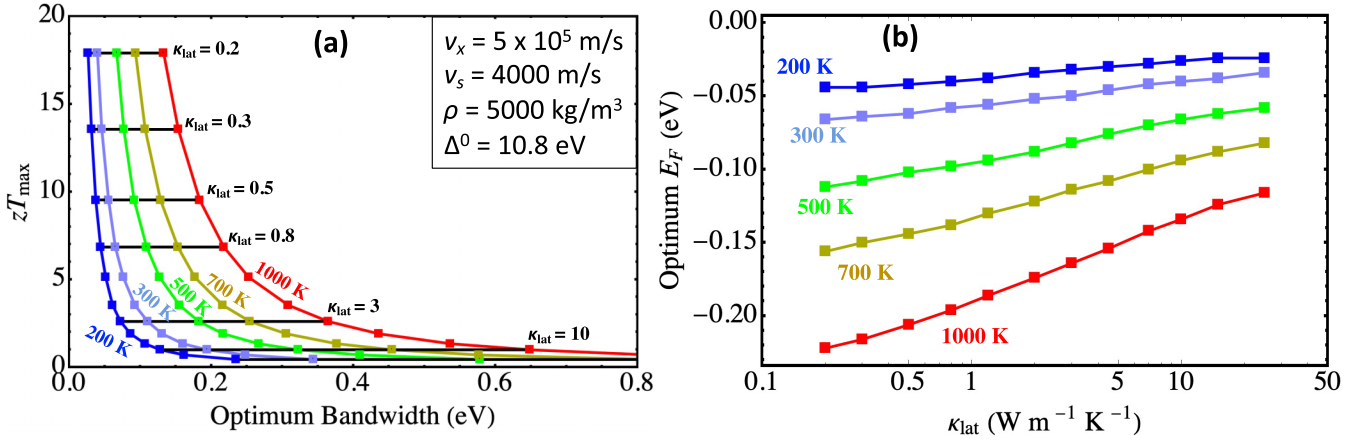FIG. 2. (a) T-and-κ_{lat}-dependent optimum bandwidth and zT under deformation-potential scattering for an isotropic three-dimensional linear band with $v_x = 5 \times 10^5$ m/s, which is the group velocity of a parabolic band with effective mass 0.067 (approximately that of GaAs) 0.1 eV above the band edge. All other material parameters are kept identically to the analysis in Ref. [23]. The κ_{lat} values are given in W m^{-1} K^{-1}. (b) Optimum Fermi level (electron chemical potential) for each case.

$W_{\text{opt}} = \operatorname{argmax}_W zT(W)$ where

$$zT(W) = \frac{\left[\int_0^W (E_{\text{F}} - E)\Sigma(E)\left(-\frac{\partial f}{\partial E}\right)dE\right]^2}{\int_0^W \Sigma(E)\left(-\frac{\partial f}{\partial E}\right)dE\left[T\kappa_{\text{lat}} + \int_0^W (E_{\text{F}} - E)^2 \Sigma(E)\left(-\frac{\partial f}{\partial E}\right)dE\right] - \left[\int_0^W (E_{\text{F}} - E)\Sigma(E)\left(-\frac{\partial f}{\partial E}\right)dE\right]^2}, \quad (2)$$

and τ is calculated using Eq. (1) and

$$\tau(E) = \frac{\rho v_s^2}{\pi k_{\text{B}} T} \frac{D^{-1}(E)}{(\Delta^0 + \langle \mathbf{v} \otimes \mathbf{v}\rangle)^2}, \quad (3)$$

where v_s is the sound velocity, ρ is the mass density, and $\langle \mathbf{v} \otimes \mathbf{v}\rangle = \langle v_x^2(E)\rangle = v_x^2$ for an isotropic linear band. For the sake of comparison with previous results for a parabolic band [23], the same material parameters are maintained. Three noteworthy observations are made here.

(1) Linear dispersion prescribed with optimized width indeed outperforms parabolic dispersion of comparable velocity and optimized width. The improvement is particularly pronounced at low temperatures. At 200 K, linear dispersion with W_{opt} yields nearly five times higher zT than the parabolic counterpart. In fact, zT_{max} is identical for all temperatures for a given κ_{lat} value and is in excellent agreement with the analytically derived results of Ref. [4] purely from boxcar $\Sigma(E)$. For $\kappa_{\text{lat}} = 0.2$ W m^{-1} K^{-1}, we have $\frac{\kappa_{\text{lat}}}{k_{\text{B}}^2 T \Sigma^\dagger} \approx 0.0209$ which is temperature independent due to the T^{-1} factor in $\Sigma^\dagger$ through Eq. (3). This quantity converts to $zT_{\text{max}} \approx 18$ both analytically and by the present calculation. This is the highlight for truly optimized band structures: the electronic performance is temperature independent, and the temperature dependence of zT is owed solely to that of κ_{lat}. A band's linearity and its bandwidth optimization are thus critical for low temperatures notoriously barren of high zT.

(2) W_{opt} for a linear band is roughly half that of a parabolic band with a similar velocity. This is ascribed to the $\Sigma(E) \propto E^0$ trend, which is much less needy of high-energy states to drive thermopower than the $\Sigma(E) \propto E^1$ trend of a parabolic band. It thus becomes more beneficial to trim high-energy contributions, sacrificing a bit of thermopower in exchange

for reducing electronic thermal conductivity, which naturally narrows W_{opt} with appropriate adjustment in E_{F}.

(3) For an isotropic linear dispersion under Eq. (3),

$$\Sigma^\dagger = \frac{\rho v_s^2}{V \pi k_{\text{B}} T} \frac{v_x^2}{\left(\Delta^0 + v_x^2\right)^2}, \quad (4)$$

meaning there is an optimum velocity for maximizing $\Sigma^\dagger$ and by default zT, precisely at $v^2 = \Delta^0$, or $v = \sqrt{\Delta^0}$. For $\Delta^0 = 10$ eV, this corresponds to $v \approx 1.32 \times 10^6$ m/s which turns out to be close to the Fermi velocity of graphene. Any higher velocity will, insofar as the Kahn-Allen potential is valid, in fact lower zT. At 300 K, W_{opt} for this velocity with $\kappa_{\text{lat}} = 0.2$ W m^{-1} K^{-1} is approximately 30 meV in theory, though realistically closer to 50 meV if not higher depending on the maximum optical phonon energy whose deformation causes inelastic scattering, and translates to $zT_{\text{max}} \approx 32$.

IV. DISCUSSIONS

Of note, Ref. [24] derives that $\Sigma(E) \propto \delta$ is optimal. This is in fact precisely the limit $W_{\text{opt}} \to 0$ as either $\kappa_{\text{lat}} \to 0$ or $v \to \infty$. However, $\kappa_{\text{lat}} \to 0$ is unrealistic in real solids, and $v \to \infty$ is at odds with the band turning completely flat such that $\Sigma(E) \propto \delta$ is possible. In fact, $v \to 0$ for a flat band, yielding zero conductivity and zero power, failing to deliver nonzero zT unless in the unrealistic case of $\kappa_{\text{lat}} \to 0$. In theory, even if $\kappa_{\text{lat}} \to 0$ were possible in which case $zT \to \infty$ and the Carnot efficiency is reached, it would only represent an extremely slow, reversible process that virtually does not occur, to no engineering relevance. These have been pointed out by multiple works in the past [1,2,4,23,25]. In practice, even a completely localized charge may be able to move via small-polaronic activated hopping, as occurs in
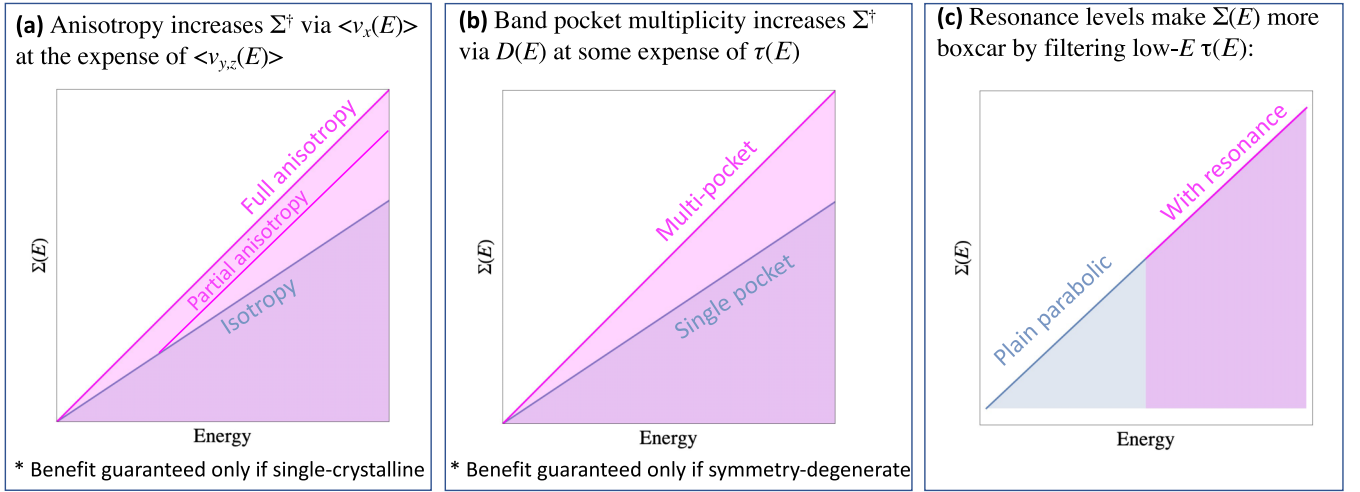
FIG. 3. Schematics of the effects of (a) band anisotropy, (b) band multiplicity, and (c) resonance levels on the $\Sigma(E)$ profile of a parabolic band, whose basic trend under deformation-potential scattering is $\Sigma_x(E) = \Sigma^\dagger E$ due to $\langle v_x^2(E)\rangle \propto E$. Notice that their benefits come by either increasing $\Sigma^\dagger$ or by making $\Sigma(E)$ more boxcar in shape.

molecular crystals [26], allowing for nonzero conductivity, power, and zT alike. Unfortunately, the mobility resulting from this mechanism is generally so low ($\mu \lesssim 10^{-2}$ cm^2 V^{-1} s^{-1}) that conductivity of at most $\sigma \approx 10^3$ S m^{-1} can be expected at a very high, metallic carrier concentration of 10^{22} cm^{-3}. This conductivity is so low that, even when paired with a very high Seebeck coefficient of 300 μV K^{-1} and the lowest practically imaginable value of $\kappa_{\text{lat}} \approx 0.1$ W m^{-1} K^{-1}, the resulting zT is less than 0.5 at 300 K. This is clearly far from optimal. Therefore, the bandwidth must conclusively be finite and optimized, with the transport mechanism remaining high-velocity band motion.

Further, the linear-band carriers within W_{opt} must not inelastically scatter into the heavy states at the cutoffs, which would drastically reduce τ everywhere to reduce $\Sigma^\dagger$ and zT. This means, given a material-dependent maximum phonon energy ω_{max} that couples inelastic scattering, which is typically on the order of 10 meV, that $W_{\text{opt}}^* = W_{\text{opt}} + \omega_{\text{max}}$ if heavy states exist on only one side [Fig. 1(b)] and $W_{\text{opt}}^* = W_{\text{opt}} + 2\omega_{\text{max}}$ if heavy states exist on both sides [Fig. 1(c)]. These would allow preservation of constant $\Sigma(E)$ with width W_{opt}, but with the boxcar edges broadening and slanting due to the inelastic effects, rendering the whole profile somewhat trapezoidal. To minimize the effect of inelasticity in practice, ω_{max} must be as small as possible, i.e. the material must be as soft as possible.

The present viewpoint also unifies the microscopic mechanisms by which other band structure features improve zT, namely, band anisotropy, band multiplicity, and resonance levels, whose salient effects have been systematically investigated in Refs. [14,23]. In short, they all improve zT via either making $\Sigma(E)$ more boxcar in shape or increasing its magnitude $\Sigma^\dagger$. Figure 3 graphically summarizes each case for a parabolic band as an example, which has a $\Sigma(E) = \Sigma^\dagger E$ profile (linear in E) under deformation-potential scattering due to $\langle v_x^2(E)\rangle \propto E$.

As Fig. 3(a) shows, band anisotropy steepens $\Sigma(E)$, i.e., increases $\Sigma^\dagger$ by steepening $\langle v_x^2(E)\rangle$ due to the low-dimensional effect, though where the steepening occurs depends on the

degree of anisotropy [23]. Anisotropy also increases $D(E)$, but this is largely if not entirely canceled by reduction in $\tau(E)$ under deformation-potential scattering.

As Fig. 3(b) paints the picture, band multiplicity also steepens $\Sigma(E)$, i.e., increases $\Sigma^\dagger$, but through the enhancement of $D(E)$ relative to the reduction in $\tau(E)$ due to interband/intervalley scattering. Because scattering between bands/valleys located at distant points in the **k** space is generally weaker than intraband/intravalley scattering [14,23], scattering does not increase as much as $D(E)$ does in the presence of multiple band pockets. For instance, if $D(E)$ increased by a factor of 2, $\tau(E)$ would decrease but by less than half, leading to an overall increase in $\Sigma^\dagger$ by a factor less than 2. Regardless, the $\tau^{-1}(E) \propto D(E)$ and $\Sigma(E) \propto \Sigma^\dagger E$ profiles are expected to persist under deformation-potential scattering.

Finally as Fig. 3(c) shows, resonance levels benefit zT by rendering $\Sigma(E)$ more boxcar in shape. By filtering out low-energy carriers via resonance scattering, it forms a steep edge in the $\Sigma(E)$ profile. Macroscopically, this has the effect of reducing the Ohmic conductivity relative to the thermoelectric conductivity, thereby enhancing the Seebeck coefficient. In fact, this is precisely the strategy to prescribe the boxcar edges depicted in Fig. 1(c), not only at low energies but also at high energies in order to curtail κ_e. Of course, the ultimate ingredient to perfecting the boxcar is a flat Σ profile in between the edges, which is delivered by linear bands under scattering by phonon deformation, coming back full circle.

V. CONCLUSION

In summary, Fig. 1(b) depicts a band structure shape that would generate a boxcar transport distribution under scattering by (acoustic) phonon deformation. The likelihood of achievement put aside, it is a qualitative optimal limit of a band structure in a realistic system that is physically conceivable and potentially closely emulatable. Figure 1(c) depicts an alternative such design suiting semimetals where linear dispersion is common and deformation-potential

scattering is nearly always dominant. Realizing the narrow optimum bandwidth would thus likely be the greatest challenge. Even if no system realizes it as far as to the ideal limit, known thermoelectric materials stand to potentially benefit from engineering the transport distribution such that it becomes more boxcarlike. The determination of linear dispersion as the optimal shape delivering a boxcar transport distribution completes the study of Ref. [23] that identified multiple band structure features that optimize zT with the exception of its qualitative shape. Given now the ideality of linear dispersion under deformation-potential scattering, one with velocity approaching $\sqrt{\Delta^0}$ and symmetry degeneracies (more carriers and/or less scattering) would lead to higher $\Sigma^\dagger$, while well-tuned bandwidth and Fermi level would optimize the Boltzmann transport integrals. This would systematically and globally maximize zT, to the benefit in particular of low-temperature performance integral to spacecraft propulsion and refrigeration.

[1] R. S. Whitney, Most Efficient Quantum Thermoelectric at Finite Power Output, Phys. Rev. Lett. **112**, 130601 (2014).

[2] R. S. Whitney, Finding the quantum thermoelectric with maximal efficiency and minimal entropy production at given power output, Phys. Rev. B **91**, 115425 (2015).

[3] Z. Fan, H.-Q. Wang, and J.-C. Zheng, Searching for the best thermoelectrics through the optimization of transport distribution function, J. Appl. Phys. **109**, 073713 (2011).

[4] J. Maassen, Limits of thermoelectric performance with a bounded transport distribution, Phys. Rev. B **104**, 184301 (2021).

[5] F. Seitz, On the mobility of electrons in pure non-polar insulators, Phys. Rev. **73**, 549 (1948).

[6] M. Lundstrom, *Fundamentals of Carrier Transport* (Cambridge University Press, Cambridge, UK, 2000).

[7] D. Rode, Low-field electron transport, in *Semiconductors and Semimetals*, edited by R. K. Willardson and Albert C. Beer (Academic Press, New York, 1975), pp. 1–89.

[8] B. Nag, *Electron Transport in Compound Semiconductors* (Springer, New York, 1980).

[9] J. M. Radcliffe, On lattice scattering in homopolar semiconductors, Proc. Phys. Soc. A **68**, 675 (1955).

[10] J. M. Ziman, *Electrons and Phonons: The Theory of Transport Phenomena in Solids* (Oxford University Press, New York, 1960).

[11] F. S. Khan and P. B. Allen, Deformation potentials and electron-phonon scattering: Two new theorems, Phys. Rev. B **29**, 3341 (1984).

[12] J. Bardeen and W. Shockley, Deformation potentials and mobilities in non-polar crystals, Phys. Rev. **80**, 72 (1950).

[13] A. M. Ganose, J. Park, A. Faghaninia, R. Woods-Robinson, K. A. Persson, and A. Jain, Efficient calculation of carrier scattering rates from first principles, Nat. Commun. **12**, 2222 (2021).

[14] J. Park, M. Dylla, Y. Xia, M. Wood, G. J. Snyder, and A. Jain, When band convergence is not beneficial for thermoelectrics, Nat. Commun. **12**, 3425 (2021).

[15] J. He, Y. Xia, S. S. Naghavi, V. Ozoliņš, and C. Wolverton, Designing chemical analogs to PbTe with intrinsic high band degeneracy and low lattice thermal conductivity, Nat. Commun. **10**, 719 (2019).

[16] Y. Xia, J. Park, F. Zhou, and V. Ozoliņš, High Thermoelectric Power Factor in Intermetallic CoSi Arising from Energy Filtering of Electrons by Phonon Scattering, Phys. Rev. Appl. **11**, 024017 (2019).

[17] C.-H. Park, F. Giustino, M. L. Cohen, and S. G. Louie, Velocity Renormalization and Carrier Lifetime in Graphene from the Electron-Phonon Interaction, Phys. Rev. Lett. **99**, 086804 (2007).

[18] Y. Xia, J. Park, V. Ozoliņš, and C. Wolverton, Leveraging electron-phonon interaction to enhance thermoelectric power factor in graphene-like semimetals, Phys. Rev. B **100**, 201401(R) (2019).

[19] B. Xu and M. J. Verstraete, First Principles Explanation of the Positive Seebeck Coefficient of Lithium, Phys. Rev. Lett. **112**, 196603 (2014).

[20] D. Chattopadhyay and H. J. Queisser, Electron scattering by ionized impurities in semiconductors, Rev. Mod. Phys. **53**, 745 (1981).

[21] E. O. Kane, Energy band structure in *p*-type germanium and silicon, J. Phys. Chem. Solids **1**, 82 (1956).

[22] E. O. Kane, Band structure of indium antimonide, J. Phys. Chem. Solids **1**, 249 (1957).

[23] J. Park, Y. Xia, V. Ozoliņš, and A. Jain, Optimal band structure for thermoelectrics with realistic scattering and bands, npj Comput. Mater. **7**, 43 (2021).

[24] G. D. Mahan and J. Sofo, The best thermoelectric, Proc. Natl. Acad. Sci. USA **93**, 7436 (1996).

[25] J. Zhou, R. Yang, G. Chen, and M. S. Dresselhaus, Optimal Bandwidth for High Efficiency Thermoelectrics, Phys. Rev. Lett. **107**, 226601 (2011).

[26] H. Oberhofer, K. Reuter, and J. Blumberger, Charge transport in molecular materials: An assessment of computational methods, Chem. Rev. **117**, 10319 (2017).